Volume 6

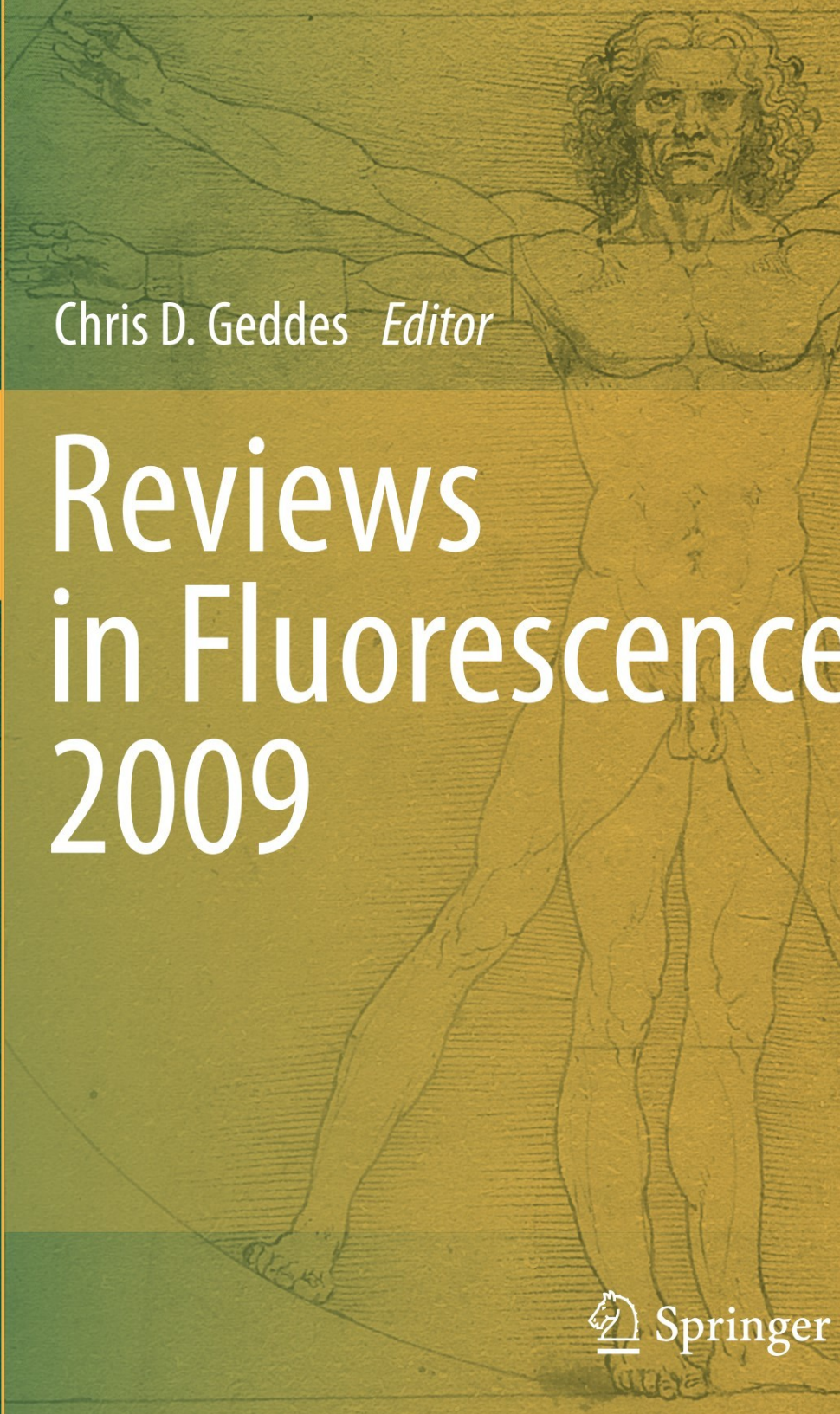

Chris D. Geddes *Editor*

Reviews in Fluorescence 2009

Springer

Reviews in Fluorescence

Editor:
Chris D. Geddes

For further volumes:
http://www.springer.com/series/6946

Chris D. Geddes
Editor

Reviews in Fluorescence 2009

Springer

Editor
Chris D. Geddes
Institute of Fluorescence
University of Maryland
701 E. Pratt St.
Baltimore, MD 21202
Suites 3017-21
USA
geddes@umbc.edu

Joseph R. Lakowicz
Center for Fluorescence Spectroscopy
725 Lombar Street
Baltimore, MD 21201
USA

ISSN 1573-8086
ISBN 978-1-4419-9671-8 e-ISBN 978-1-4419-9672-5
DOI 10.1007/978-1-4419-9672-5
Springer New York Dordrecht Heidelberg London

Preface

This is the sixth volume in the *Reviews in Fluorescence* series. To date, five previous volumes have been both published and well-received by the scientific community. Several book reviews, in the last few years, have also favorably remarked on the series.

We thank the authors for their very timely and exciting contributions again this year. We hope you will find this volume as useful as past volumes, which promises to be just as diverse with regard to fluorescence-based content.

Finally, in closing, I would like to thank Caroleann Aitken, Manager, The Institute of Fluorescence, for help in coordinating content with authors and Michael Weston at Springer for help in publishing this current volume.

Chris D. Geddes

Contents

Contributors

Martin Štefl J. Heyrovský Institute of Physical Chemistry v.v.i., Academy of Sciences of the Czech Republic, Dolejškova 3, Prague 18223, Czech Republic

J.R. Albani Laboratoire de Biophysique Moléculaire, Université des Sciences et Technologies de Lille, Bâtiment C6. 59655, Villeneuve d'Ascq Cédex, France

Wajih Al-Soufi Departamento de Química Física, Facultade de Ciencias, Universidade de Santiago de Compostela, E-27002 Lugo, Spain

Jon P. Anderson LI-COR Biosciences Inc., 4647 Superior Street, Lincoln, NE 68504, USA

Andrea Balogh Department of Immunology, Eötvös Lorand University, Pazmany Peter setany 1/C, 1117 Budapest, Hungary

Buddhudu Srinivasa Department of Physics, Sri Venkateswara University, Tirupati 517502, Andhra Pradesh, India

Peter J. Butler Department of Bioengineering, The Pennsylvania State University, 205 Hallowell Building, University Park, PA 16802, USA

Zhi Cao Department of Chemistry, New Mexico Institute of Mining and Technology, Socorro, NM 87801, USA

Nihav Dhawale School of Physical Sciences, Jawaharlal Nehru University, New Delhi 110 067, India

Tarek A. Fayed Chemistry Department, Faculty of Science,
Tanta University, 31527 Tanta, Egypt

Michael C. Ferko Stryker Orthopaedics, 325 Corporate Drive,
Mahwah, NJ 07430, USA

Daniel L. Grone LI-COR Biosciences Inc., 4647 Superior Street,
Lincoln, NE 68504, USA

Ramachandra R. Gullapalli Department of Bioengineering,
The Pennsylvania State University, 205 Hallowell Building,
University Park, PA 16802, USA

Michael D. Heagy Department of Chemistry, New Mexico Institute
of Mining and Technology, Socorro, NM 87801, USA

Martin Hof J. Heyrovský Institute of Physical Chemistry v.v.i.,
Academy of Sciences of the Czech Republic, Dolejškova 3,
Prague 18223, Czech Republic

G. Krishnamoorthy Department of Chemical Sciences,
Tata Institute of Fundamental Research, Mumbai 400 005, India

Sakari Kulmala School of Chemical Technology,
Aalto University, Espoo, Finland

Bhaskar Kumar Grandhe Department of Physics,
Sri Venkateswara University, Tirupati 517502, Andhra Pradesh, India

Radek Macháň J. Heyrovský Institute of Physical Chemistry v.v.i.,
Academy of Sciences of the Czech Republic, Dolejškova 3,
Prague 18223, Czech Republic

János Matkó Department of Immunology, Eötvös Lorand University,
Pazmany Peter setany 1/C, 1117 Budapest, Hungary

Immunology Research Group of the Hungarian Academy of Sciences,
Eötvös Lorand University, Budapest, Hungary

Manuel Mosquera Departamento de Química Física,
Facultade de Química, Universidade de Santiago de Compostela,
E-15782 Santiago de Compostela, Spain

Péter Nagy Department of Biophysics and Cell Biology,
University of Debrecen, Debrecen, Hungary

Premchendar Nandhikonda Department of Chemistry, New Mexico Institute of Mining and Technology, Socorro, NM 87801, USA

Punya Navaratnarajah Department of Biochemistry and Biophysics, University of North Carolina at Chapel Hill, Chapel Hill, NC 27599-7260, USA

Michael G. Nichols Physics Department, Creighton University, 2500 California Plaza, Omaha, NE 68178, USA

Mercedes Novo Departamento de Química Física, Facultade de Ciencias, Universidade de Santiago de Compostela, E-27002 Lugo, Spain

Flor Rodríguez-Prieto Departamento de Química Física, Facultade de Química, Universidade de Santiago de Compostela, E-15782 Santiago de Compostela, Spain

Saswata Sankar Sarkar Department of Chemical Sciences, Tata Institute of Fundamental Research, Mumbai 400 005, India

Anoop Saxena Department of Chemical Sciences, Tata Institute of Fundamental Research, Mumbai 400 005, India

Alexander Schiller Institute for Inorganic and Analytical Chemistry, Friedrich-Schiller-University Jena, Humboldtstr. 8, 07743 Jena, Germany

Bakthan Singaram Department of Chemistry and Biochemistry, University of California, 1156 High Street, Santa Cruz, CA 95064, USA

Johanna Suomi School of Chemical Technology, Aalto University, Espoo, Finland

János Szöllősi Cell Biology and Signaling Research Group of the Hungarian Academy of Sciences, University of Debrecen, Debrecen, Hungary

Tristan Tabouillot Department of Bioengineering, The Pennsylvania State University, 205 Hallowell Building, University Park, PA 16802, USA

Nancy L. Thompson Department of Chemistry, University of North Carolina at Chapel Hill, Chapel Hill, NC 27599-3290, USA

Department of Biochemistry and Biophysics, University of North Carolina at Chapel Hill, Chapel Hill, NC, USA

Jayant B. Udgaonkar National Centre for Biological Sciences, Tata Institute of Fundamental Research, Bangalore 560 065, India

Boaz Vilozny Department of Chemistry and Biochemistry, University of California, 1156 High Street, Santa Cruz, CA 95064, USA

Xiang Wang Department of Chemistry, University of North Carolina at Chapel Hill, Chapel Hill, NC 27599-3290, USA

Ritchie A. Wessling Department of Chemistry and Biochemistry, University of California, 1156 High Street, Santa Cruz, CA 95064, USA

John G. Williams LI-COR Biosciences Inc., 4647 Superior Street, Lincoln, NE 68504, USA

Metal Enhancement of Near-IR Fluorescence for Molecular Biotechnology Applications

Jon P. Anderson, John G. Williams, Daniel L. Grone, and Michael G. Nichols

Abstract Metal-enhanced fluorescence (MEF) can increase the overall emissions of a multitude of fluorophores by positioning the fluorophore in close proximity to an appropriate metal-coated surface. Near-infrared (near-IR) fluorophores placed near these metal surfaces combine the increased emissions of MEF with the low background characteristics of near-IR fluorescence. Together, this combination of high emission, low background detection may provide a powerful tool in the analysis of biological samples. In this brief review, we will outline the feasibility of using near-IR MEF in biotechnology research, will cover the types of experiments required to bring this technology from the feasibility stage to a commercial product, usable by molecular biologists, and will investigate the sources of background emissions that may be further reduced in the future.

1 Introduction

Fluorescence is a highly sensitive and convenient method of detection that has altered the landscape of molecular biotechnology over the past few decades. An increasingly wide variety of fluorophores are used in biotechnology, genomics, immunoassays, array technologies, imaging, and drug discovery [11, 32, 60, 61, 69]. Fluorescent molecules can easily be attached to a cast of target molecules, including DNA, RNA, antibodies, peptides, and proteins, and have the distinct advantage of being small compared to several other molecular labels [16, 20, 62, 71, 73]. Fluorescence-based technologies are used in a wide variety of biotechnology applications, including automated DNA sequencing, real-time PCR, microarray analyses, and immunoassays. The small size of fluorescent dyes provides little interference with the properties of the labeled molecule and allows the dye to

J.P. Anderson (✉)
LI-COR Biosciences Inc., 4647 Superior Street, Lincoln, NE 68504, USA
e-mail: jon.anderson@licor.com

C.D. Geddes (ed.), *Reviews in Fluorescence 2009*, Reviews in Fluorescence 2009,
DOI 10.1007/978-1-4419-9672-5_1,

infiltrate cellular regions that cannot be labeled by larger molecules (i.e., quantum dots and metal colloids) [14, 63]. Fluorescent dyes provide a predictable red-wavelength Stokes shift from the excitation to the emission spectra, allowing for very efficient collection of the emission photons away from the excitation beam [14, 52]. In addition to measuring the excitation wavelength, fluorescence can provide information by the way of polarization, lifetime, fluorescence resonance energy transfer (FRET), and quenching. Discovery and development of green fluorescent protein (GFP) has also allowed for the direct labeling and expression of a fluorescent biomolecule by a protein [12]. A major drawback, however, in using fluorescent dyes is the fact that the dyes can easily photodegrade, unlike quantum dots and metal colloids. Fluorescent molecules with small Stokes shifts may also have the disadvantage of self-quenching when located near another fluorophore by means of homo-FRET, reducing the overall signal.

Near-infrared (near-IR)fluorescence has unique advantages over visible fluorescence and is gaining popularity in biological imaging and molecular applications [64]. Fluorescence in the near-IR offers significantly lower background signals from scatter than those generated by visible wavelength excitation [50, 55]. Near-IR wavelengths are not readily absorbed by water and biological compounds, allowing deep penetration through tissues and cells, and reducing the possibility of photodamage to biological samples. Instruments using these longer wavelengths have a distinct advantage, with the near-IR spectral region showing little interference from biological molecules [51, 65].

2 Metal-Enhanced Fluorescence

Though highly successful, fluorescent-based methodologies have a continuing need for increased sensitivity and reduced detection limits [34]. To improve the sensitivity and reliability of fluorescent probes, the signal emissions from target molecules need to increase without increasing the signal from nonspecific molecules. In other words, the sensitivity and detection limit can be improved by increasing the quantum yield of the fluorophore, increasing its absorption cross section, increasing its photostability, and reducing the background signal of the system.

Metal-enhanced fluorescence (MEF) has been highly successful at increasing fluorescence sensitivity through an increase of the quantum yield and photostability of the fluorophore [4, 7, 35, 36]. The act of using a metal-coated surface to increase signal intensities is not a recent endeavor, for metal island films have been used for over two decades in Raman spectroscopy for signal enhancement [1, 17]. However, this field has only recently begun to show a large following in the field of fluorescence detection [35, 37, 40, 44, 47, 48]. Research on MEF has primarily focused on using silver island films (SIFs) [3, 5, 38, 40, 45, 46, 48] for enhancement of fluorescence, although recent studies have utilized metal colloids [6, 43], light-deposited silver [23], silver fractals [24], nanosphere lithography [29], and ordered arrays [15]. SIFs are composed of subwavelength sized patches of silver

located on an inert substrate. Randomly seeded metal islands that ranged in size from 20 to 500 nm have been successfully used to enhance a variety of fluorophores [38, 40, 45, 46, 48]. The size and the shape of the metal islands may also play an important role in the ability to enhance the fluorescent signal [26, 59]. Periodic metal island nanoarray structures may further enhance the fluorophore emissions and could result in directional instead of isotropic photonic emissions [37].

SIFs have been largely studied for their ability to increase fluorescence intensities in low quantum yield and visible fluorophores [28, 40, 44, 45]. Much less information, however, exists on the ability of these metal islands to enhance the performance of the longer-wavelength, near-IR fluorophores commonly used in proteomic and genomic applications. The combination of increased emissions from MEF and the low background signal from near-IR fluorescence provides a means for lowering the limit of detection (LOD), providing the increased sensitivity that is required for many biological assays.

3 MEF Design Considerations

In MEF, the distance between the fluorophore and the metal is critical for enhancement of fluorescent emissions. The metal will quench the fluorophore if it is located within 50 Å of the metal surface. At a distance greater than 200 Å from the metal surface, the fluorophore displays free space characteristics. Therefore, the fluorophore must be located roughly between 50 and 200 Å from the metal surface for metal enhancement to take place (Fig. 1). It is this nanometer sized zone of enhancement that provides the greatest effect to a fluorophore's quantum yield and may aid in signal specificity, essentially amplifying only those fluorophores that are specifically located within this enhancement zone.

Metallic surfaces placed near a fluorophore can alter the fluorophore's properties. MEF uses metallic surfaces to modify the radiative decay rate (Γ) in a

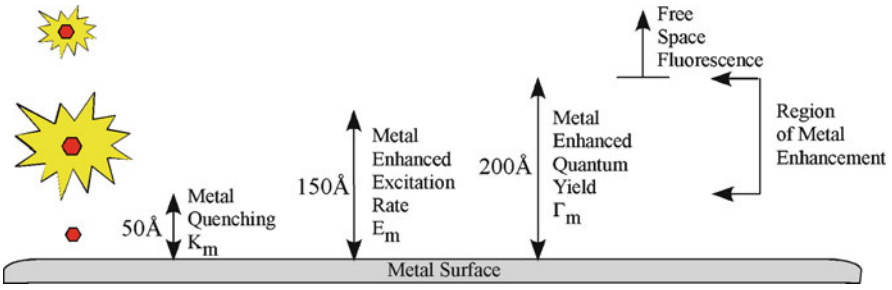

Fig. 1 Schematic representation of fluorescent properties near a metal surface. MEF properties are shown, as the particle moves from near the surface where it is quenched by the metal, through the region of metal enhancement and then into free space, where the metal has no effect on the particle

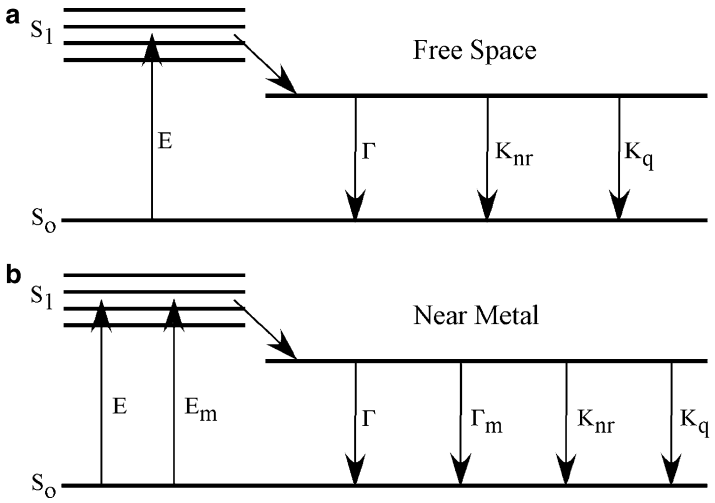

Fig. 2 Simplified Jablonski diagram showing fluorophores in (**a**) free space and (**b**) in the presence of a metallic nanoparticle. The diagram highlights the radiative decay rate (Γ), the radiative decay rate in the presence of metal nanoparticles (Γ_m), the nonradiative decay rate (k_{nr}), and the rate of quenching processes (k_q)

useful manner [35, 40]. An excited fluorophore can emit or return to a ground state by means of some nonradiative decay at a rate (k_{nr}) or by other quenching processes at a rate (k_q) (Fig. 2a). Fluorophores placed near a metal show both a decreased lifetime and an increased quantum yield, indicating an effect on Γ (Fig. 2b). Alterations in Γ are due to interactions of the excited state fluorophores with the oscillations of the free electrons in the metal [18, 33, 40]. The excited fluorophores induce surface plasmons which in turn emit photons [9, 49]. The fluorescence lifetime (τ_m) and the quantum yield (Q_m) for a fluorophore placed near a metal surface are given by the equations:

$$\tau_m = \frac{1}{\Gamma + \Gamma_m + k_{nr} + k_q}, \tag{1}$$

$$Q_m = \frac{\Gamma + \Gamma_m}{\Gamma + \Gamma_m + k_{nr} + k_q}. \tag{2}$$

By reducing the lifetime and increasing the quantum yield, metallic surfaces may increase the overall radiative rate of a fluorophore by more than 10,000-fold [33], although this increase is greatest for low quantum yield fluorophores [40]. Naturally, high quantum yield fluorophores may reveal only moderate gains in the overall quantum yield when placed near a metal surface; however, these dyes may still show a decrease in their fluorescent lifetime [40]. Producing a decrease in the

fluorescence lifetime near a metal surface can result in a greater number of total photons emitted and an increased photostability. The maximum number of photons emitted by a fluorophore per second is limited by the inverse of the lifetime. The photostability of the fluorophore is affected by the amount of time the fluorophore remains in the excited state, where it may photodegrade. By reducing the lifetime (i.e., the average time spent in the excited state), the fluorophore can effectively pass through more excitation-emission cycles and thus produce an increased number of photons before photodegrading.

Though MEF has been successfully demonstrated by multiple groups [18, 26, 33, 40], there remains little experimental data on the effects of MEF on near-IR fluorescence. Furthermore, even with the successful demonstration of this technology, there still remain several challenges in transferring this technology from the research stage to the commercial stage. The process of demonstrating feasibility using MEF is only the first stage in making this technology useful for molecular biologists. Studies on the reproducibility and linearity of the fluorescence emissions, along with investigations on the longevity of theses metal structures, need to be performed before they can be reliably used to quantitate labeled biological samples. Along with these verification studies, a fundamental understanding of the sources of background will help find ways to reduce noise in the assay and lower the LOD beyond current methodologies.

4 Silver Island Films

Preliminary results with LI-COR IRDye®800CW (ex 774 nm; em 789 nm) showed that near-IR fluorophores can be enhanced by both silver and gold nanostructures. The silver structures were shown to enhance the dye significantly more than the gold, a result that is not unexpected and has been reported for visible fluorophores [49]. From these initial results, we decided to focus on silver structures and proceeded to produce silver coatings on glass slides, including SIFs and colloid-coated surfaces.

Experiments were performed to quantitate the relative enhancement of near-IR fluorophores on the deposited silver-coated glass surface as compared to the uncoated glass. Throughout our experiments, a known quantity of fluorophore-labeled protein or DNA was spotted onto the SIF-coated and uncoated portions of the glass slides and then detected using a LI-COR Odyssey® near-IR fluorescence imager (Fig. 3). Spotting a known amount of fluorophore onto the SIF-coated or uncoated glass surface allows us to remove any affinity biases that may occur when depositing a layer of fluorophores over the entire surface of a slide. Analyzing individual spots on a scanned image also allows the Odyssey® software to account for any increase in background fluorescence signal caused by the silver surface, with the near-IR excitation wavelengths producing almost no increase in the background signal.

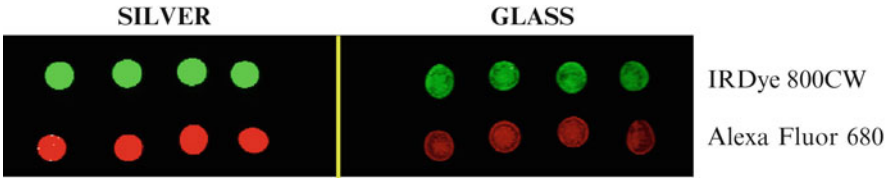

Fig. 3 Typical results of fluorophore enhancement by SIF. Equal amounts of LI-COR IRDye®800 (*green*) and Molecular Probes Alexa Fluor® 680 (*red*) labeled streptavidin are spotted onto either the silver-coated (SILVER) or uncoated (GLASS) regions of a glass slide and allowed to dry. The slide is imaged using a LI-COR Odyssey® imager. The SIF-coated regions show increased fluorescence intensity as shown by the brighter spots

4.1 Fluorophore to SIF Distance Dependence

The distance between the fluorophore and the SIF is critical for metal enhancement to take place. Previous studies have concluded that at distances greater than 30–50 nm from the SIF, the fluorophore and metal surface generate little measurable interaction and the fluorophore displays mainly free space characteristics [46]. When the fluorophore is in close proximity to the metal surface, however, the excited fluorophore induces surface plasmons in the SIF, which then also radiate at the same wavelengths as the excited state fluorophore [13]. Using both LI-COR IRDye®700 (ex 689 nm; em 700 nm) and IRDye®800 near-IR fluorophore-labeled oligos, we observed this distance-dependent relationship by spotting 1 μl (10 fmol) of dye-labeled DNA oligo onto the SIF-coated and uncoated portions of the glass slide, and detecting the fluorescence emissions generated from each droplet as it dried. The drying of the droplet moved the dye-labeled DNA oligos from a free space emission mode, far from the SIF surface, to a metal-enhanced mode, near the SIF surface (Fig. 4). Integrated intensities were measured for each of the spots and the relative amount of enhancement for fluorophores spotted over silver was calculated. The integrated intensity calculations on the Odyssey® system are independent of the spot size and scan resolution, and account for any increased background signal generated by the silver surface [42]. Measured over time as the spot dried, signal from dye-labeled oligos spotted on an uncoated region of the glass slide showed little change, while oligos spotted on the SIF-coated region of the slide showed increased fluorescence emissions.

SIFs are generated by a chemical reduction of silver nitrate in solution [39, 40, 45–47, 59]. The process of producing the SIF creates a heterogeneous population of metal nanostructures. The size, shape, and position of the silver nanostructures are somewhat random along the glass surface (Fig. 5). By specifying the coating time, however, the size and density of the silver structures can be roughly controlled. To determine the optimal SIF density for enhancement of near-IR fluorophores, we first generated SIF gradients on glass slides. The SIF gradients were constructed by slowly retracting a glass slide from the reduced silver nitrate solution as it is heated in a 40°C waterbath. The slow removal of the slide was done by using a programmable

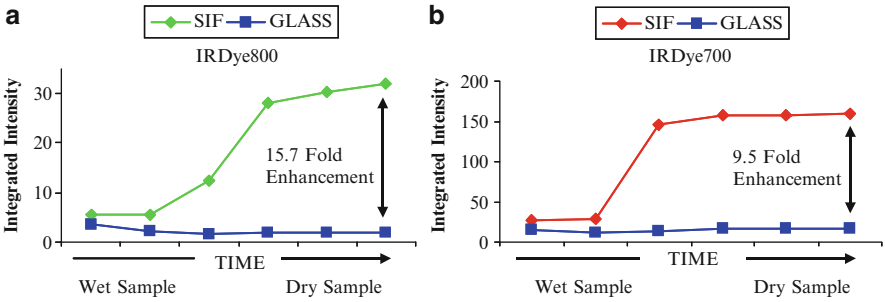

Fig. 4 Fluorescence integrated intensity of an (**a**) IRDye®800- and (**b**) IRDye®700-labeled DNA oligo spotted onto either a plain glass slide (GLASS) or onto a silver island film coated glass slide (SIF). The integrated intensity is monitored over time as the liquid spot dries onto the slide, bringing the fluorophore in close proximity to the silver surface, and producing an increase in the fluorescence intensity for the SIF sample. The data was generated by implementing consecutive scans on the Odyssey® imager, and with the focus plane of detection adjusted to accommodate for scanning through the bottom of the glass slide to allow for the imaging of wet spots

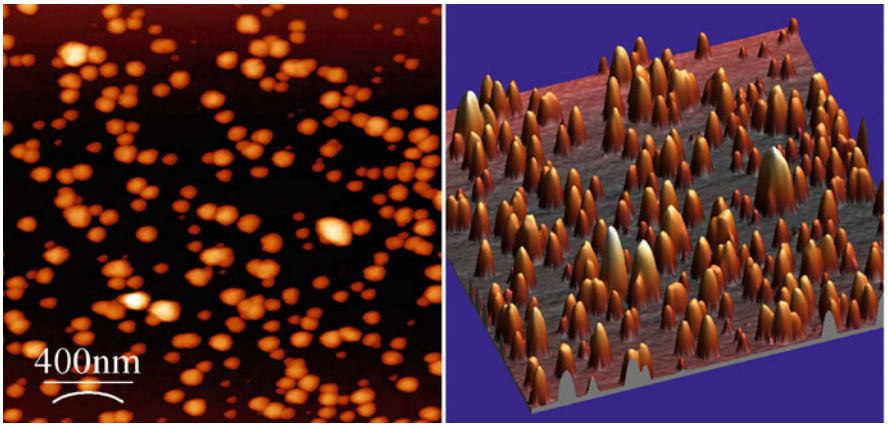

Fig. 5 Atomic force micrograph (AFM) image of a typical silver island film (SIF) produced by LI-COR and imaged at the University of Nebraska-Lincoln. Image on the *right* is a 3D reconstruction of the AFM image. Note variations in size and random distribution of silver nanostructures

stepper motor that would retract the slide from the silver solution at a rate of approximately 5 mm/min, creating a reproducible SIF gradient. Absorption spectra were taken at various regions along the SIF gradient, with the peak absorption correlating to the silver density on the slide surface. Near-IR fluorophore-labeled DNA oligos were then spotted along the SIF gradient and the emissions were recorded and analyzed using an Odyssey® imager. These experiments determined that a SIF containing a peak absorbance of 0.6–0.8 absorbance units (AU) would produce the greatest enhancement of near-IR fluorophores (Fig. 6).

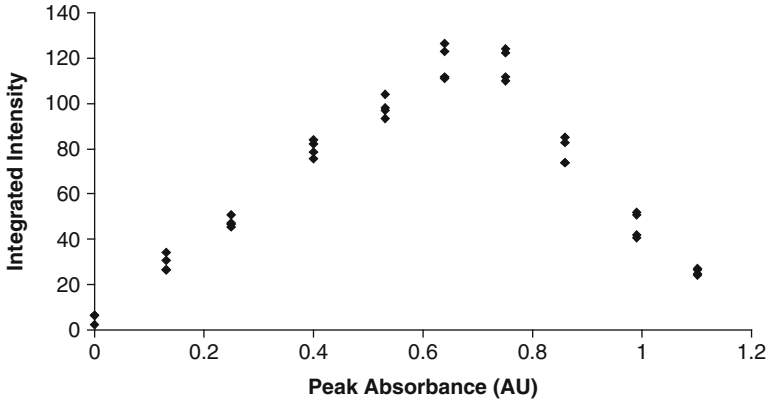

Fig. 6 A plot of the relationship between SIF coating density is shown, as measured by peak absorbance, and the integrated intensity measurement of 10 fmol of an IRDye®700-labeled DNA oligo. A total of four measurements were taken at each silver density along the SIF gradient slide. The results indicate that a SIF coating that produces an absorption intensity peak between 0.6 and 0.8 AU produced the highest integrated intensity

Using SIFs optimized for near-IR enhancement, we were able to obtain an average of 18-fold enhancement of IRDye®700-labeled DNA oligo spotted on plain glass using a manual glass slide microarrayer system (V&P Scientific inc.). IRDye®800-labeled DNA oligo was enhanced 15-fold over dye on plain glass. These enhancement results are slightly better than what has been achieved using SIFs on visible fluorophores [4, 40, 46].

5 Colloid-Coated Surfaces

Producing metal islands of a specific size may be critical for efficient MEF. Although chemical dip coating can successfully create SIFs over a range of sizes, controlling the reaction and halting the growth of the islands at an exact size and density can be difficult. Silver colloids were therefore generated to create colloid-coated surfaces containing islands of a specific size across the entire slide. The process uses metal nanoparticles (colloids) to effectively coat a glass slide, creating a metal island film. A clean glass substrate is surface coated with 3-aminopropyltrimethoxysilane (APS), producing a monolayer of reactive groups that can bind colloidal silver nanoparticles [19, 58]. The silanized glass substrates is then immersed in a colloidal solution, immobilizing the metal nanoparticles on the surface [66].

The particle spacing on the glass surface is random, with the interparticle spacing (i.e., the particle density) being dependent on both the amount of time the substrate is immersed in the colloidal solution and the concentration of the colloidal solution. Because the size of the islands is determined by the colloids, sparse to densely packed colloid-coated surfaces that maintain a unique metal island size by

simply varying the amount of time used to attach the colloids to the glass surface can be produced. This finer control of the nanostructure size and density was investigated to determine if these colloid-coated surfaces could provide even greater enhancement for near-IR fluorophores.

Reports have indicated that colloid-coated glass surfaces can enhance the fluorescence of some visible fluorophores more than SIFs, with the best results showing 16.7-fold enhancements [43]. Several methods of producing silver colloids were employed, including sodium citrate reduction [43], the polyol process using ethylene glycol as the reductant [67, 68], small silver seed production followed by repeated rounds of controlled growth [8, 10], silver reduction in the presence of gum arabic [27, 72], as well as the photoinduced production of triangular silver particles [30, 31]. Using these methodologies, we were able to generate colloids from 4 nm to greater than 120 nm in diameter. Sizes of the colloids were determined at Brookhaven Instruments Corporation (Holtsville, NY) using a Brookhaven 90Plus dynamic light scattering particle size analyzer. The colloids were attached to APS-coated glass slides by dip coating the slides for up to 24 h in the colloid solution. These various sized colloid-coated surfaces generated enhancements of up to 11-fold for IRDye®800CW and up to 5-fold for IRDye®700. These results did show enhancement by the colloid-coated surfaces, but the enhancements obtained were less than that obtained from the SIFs. The longer-wavelength, near-IR fluorescence may not be efficiently enhanced with small (4–120 nm) colloids that were tested, whereas the shorter, visible fluorescence may have been better enhanced. Producing larger colloids that are highly monodispersed might improve the enhancement for the near-IR, but we have not yet tested this hypothesis. Based on these results, we moved away from colloid-coated surfaces and began to focus our attention on characterizing the near-IR metal enhancement from SIFs.

6 Validation Tests for Near-IR MEF

Apart from demonstrating feasibility of MEF on near-IR fluorescence, we set out to further test the characteristics of the SIF-coated slides and to validate their properties. These validation tests include assays on longevity, reproducibility, and linearity.

Longevity studies involve storing SIF-coated slides for several months and then assaying them for their ability to enhance near-IR fluorescence. These shelf-life studies may not be routinely done for determining the feasibility of a product, but are crucial for the development of a commercially viable product.

SIF-coated slides are also tested for their ability to produce consistent, reproducible results across a coated slide surface. An array of near-IR fluorophore-labeled protein spots is first generated across a slide using a SpotBot personal microarrayer. Fluorescence emissions from the spots on the SIF-coated and uncoated regions of the slide are then compared, with the goal of maintaining % CV values not statistically different than that of plain glass slides.

Linearity measurements are performed on the slides to validate that the fluorescence intensities recorded by the Odyssey® scanner remain linear over several orders of magnitude based on the amount of fluorophore spotted on the slide. These types of measurements remain important to the utility of the slides as a commercial product.

6.1 Longevity of SIF-Coated Surfaces

Silver surfaces and films are prone to oxidation and are far less stable than gold surfaces [25, 75]. Frequently, SIFs are used immediately after they are produced, but have routinely be stored for up to 1 week in deionized water before being used [54]. In order to protect and stabilize the silver, others have applied a thin coating of silica to the silver surface [2, 53]. This thin layer of silica should help protect the silver surface, but could however adversely affect the ability of the SIF to enhance fluorescence by MEF. To first determine if a protective layer will be needed on the silver-coated glass slides, we performed a longevity study on the SIF-coated slides.

The longevity study was designed to measure the ability of the SIF surfaces to continue to enhance near-IR fluorophores over time. For this investigation, we generated SIF-coated slides and stored them under three different conditions for a period of 9 months. It should be noted that the stored slides were prepared before we determined the best silver density for near-IR fluorophores and contained an average peak absorbance of 0.3 AU, which is suboptimal for enhancement of near-IR fluorophores. All newly prepared SIF-coated slides that were used in the longevity study were also made with similar (0.3 AU) absorbances. The storage conditions for these slides included: wet (in dH_2O), dry under argon, and dry under ambient conditions. After 9 months, the stored slides, along with newly prepared SIF-coated slides, were freshly spotted with dye-labeled oligo and tested for their ability to enhance near-IR fluorophores. The results showed that IRDye®800-labeled DNA oligos were enhanced by an average of 6.6-fold for newly prepared slides, while the slides stored dry under Argon and Ambient conditions enhanced the dye by an average of 10.9-fold and 8.4-fold, respectively. The IRDye®700-labeled DNA oligos were enhanced by an average of 13.8-fold for newly prepared slides, while the slides stored dry under Argon and Ambient conditions enhanced the dye by an average of 4.0-fold and 4.4-fold, respectively. The slides stored for 9 months in H_2O had a visually distinct alteration in their appearance and were unable to enhance either fluorophore.

Our longevity studies demonstrated that the SIFs were able to be stored dry for 9 months and still sustain their ability to enhance the near-IR fluorophores. The reduction in the overall enhancement of these stored and newly prepared SIF-coated slides can be accounted for by the suboptimal coating of SIF, which contained an absorbance of approximately 0.3 AU. The optimal absorbance for SIF

using LI-COR dyes was later determined to be between 0.6 and 0.8 AU (Fig. 6). This difference in the amount of silver coating on the slides can generate the slightly lower enhancements that were observed in the longevity studies as compared to our best enhancements using SIFs, which were 15-fold for IRDye®800- and 18-fold for IRDye®700-labeled DNA oligos. The results, however, show that the slides stored dry remain able to effectively enhance near-IR fluorophores even after 9 months of storage, although a reduction in enhancement was observed using IRDye®700.

These results demonstrate that we may not need to overcoat the silver nanostructures with silica or other self-assembled monolayers (SAMs) to preserve their function over time. Silica or SAM coatings may, however, still be useful in providing specific surface coatings over the SIF-coated slide. Experiments on SAMs with the protein BSA have been shown to work well with silver-coated surfaces and allow for enhancement of visible fluorophores [46, 70]. Others have also performed research on overcoating silver surfaces with increasing thicknesses of silica. These results indicate that silica can be successfully used to coat the silver surfaces with a thickness of 10–15 nm silica being optimal for providing fluorescence enhancement [74].

6.2 Reproducibility of Near-IR MEF

The ability to reproducibly generate a fluorescence signal across the surface of a silver-coated glass slide is paramount in developing a commercial product. Simply producing a SIF surface that can enhance fluorescence will not be of use unless the enhancement is reproducible across the surface of the slide. Reproducibility of the silver-coated glass surfaces were determined by measuring the percent coefficient of variation (%CV) of the intensity from fluorescently labeled protein or DNA spotted along either uncoated or SIF-coated glass slides. The %CV is calculated as the standard deviation of the sample intensities divided by the mean sample intensity, multiplied by 100. For each slide that was half coated with a SIF, a SpotBot microarrayer (Telechem International Inc.) was used to spot approximately 350–450 individual spots on both the silver-coated and uncoated halves of the slide (Fig. 7). Fluorescence intensities were collected by scanning the spotted slides on an Odyssey® imaging system and analyzing the data using either Odyssey® software or Media Cybernetics Array-Pro Analyzer version 4.5 software. The fluorescence intensities from the silver-coated and uncoated portions of each slide were then used to compute %CVs. A paired *T*-test was then used to statistically analyze the silver-coated and uncoated regions of a slide. The results indicate that there was no significant difference in the %CVs for the coated and uncoated regions of the slide, with the uncoated glass maintaining an average CVs of 12.84 $\pm$ 5.28%, and the silver-coated glass having an average CV of 13.39 $\pm$ 5.41%.

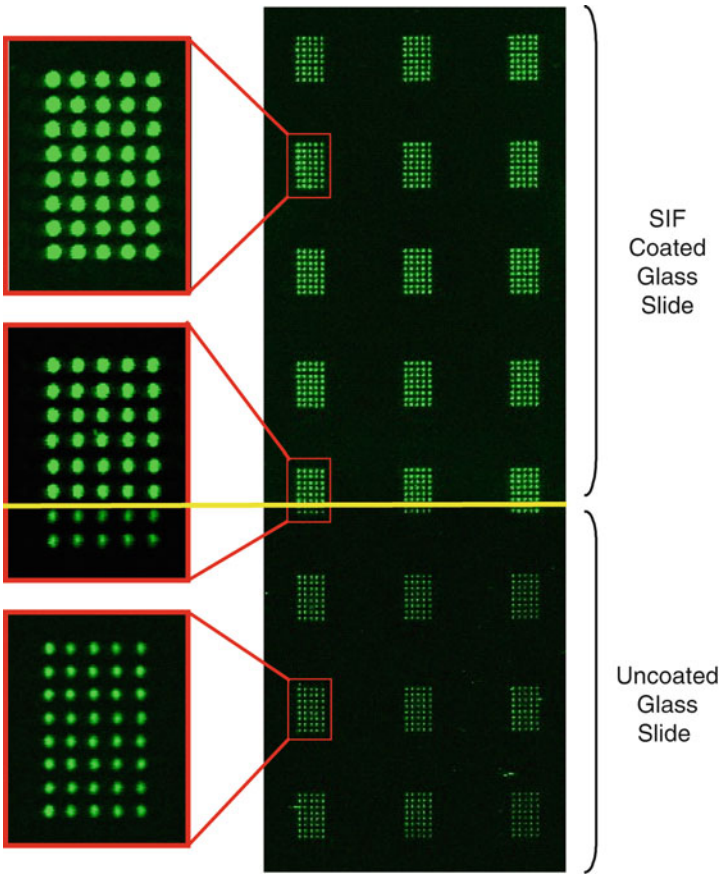

Fig. 7 Fluorescence reproducibility of SIF-coated glass slides. An Odyssey® image of a glass slide spotted with IRDye®800CW-labeled streptavidin is shown. The upper portion of the slide (above the *yellow line*) is coated with a SIF, while the lower portion of the slide is uncoated. A SpotBot personal microarrayer was used to spot grids of 40 individual spots along the glass slide, which were then analyzed using either Odyssey® or Array-Pro software. Enlarged sections of the SIF-coated region (*top*), transition region from SIF coated to uncoated (*middle*), and uncoated region (*bottom*) of the slide are shown, with fluorophores spotted over SIF-coated glass showing enhanced fluorescence signals

6.3 Linearity of Enhanced Fluorescence

The SIF-coated slides have been shown to generate up to an 18-fold increase in fluorescence emissions of near-IR dyes, but these enhancements alone cannot determine the overall utility of using SIFs in molecular biology applications. For this methodology to be a useful quantitative tool, it would be advantageous to show that the system is linear over a wide range of fluorophore concentrations. To show that SIFs can be used as a molecular biology tool for enhancing near-IR

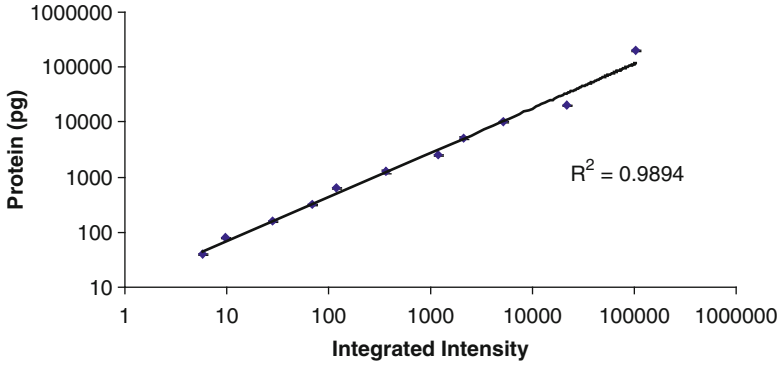

Fig. 8 Linearity of SIF fluorescence enhancement. Twofold serial dilutions of IRDye®800CW-labeled Goat-IgG antibody are plotted. Each plotted point represents the average of two measurements, with one standard deviation shown above and below the average by error bars

fluorescence, we determined the linearity of our assay over four orders of magnitude. A series of twofold serial dilutions were prepared using IRDye®800CW-labeled Goat-IgG antibody (LI-COR). The dilution series was spotted in duplicate onto a SIF-coated glass slide and imaged using an Odyssey® scanner at two intensity settings. A low-intensity setting was used to avoid saturation of fluorescence signal in concentrated sample spots and a higher scan intensity setting was used to detect highly dilute samples. The linearity measurements were performed on the slides to validate that the fluorescence intensities recorded by the Odyssey® scanner remain linear, based on the amount of fluorophore spotted on the slide. The results demonstrate that the signal is linear with dye amount over four orders of magnitude with an R^2 value of 0.9894 (Fig. 8).

7 Background Reduction

The use of MEF for producing increased fluorescence intensity has been successfully demonstrated using a variety of fluorophores [38, 40, 45, 46, 48]. However, along with the dramatic increase in signal, these metal island films may also display an increased amount of background or scatter, hindering detection of a desired signal. One of the main goals of using MEF to enhance near-IR fluorescence is the ability to significantly lower the LOD. The ability to improve the LOD can greatly expand the utility of a technique. Greater sensitivity allows the use of smaller samples, the ability to test for more analytes in a single small sample and, in the case of immunoassays, an improved LOD would expand the repertoire of available antibodies to include those with lower binding affinities.

For our experiments, the LOD is defined as the smallest concentration of analyte that can be reliably detected above the system noise, producing a signal that is three times the standard deviation (3σ) of the system noise level. Since the LOD is

directly related to the background noise level of the system, the ability of the Odyssey® to detect in the near-IR is advantageous for silver-coated slides, with the silver surfaces producing little added background signal. Any further reduction in the background, however, will aid in the reduction of the overall LOD of the system. Therefore, we set out to develop a better understanding of the sources of background coming from silver particle coated surfaces, with the aim of reducing such background and lowering the LOD.

7.1 Silver Storms

One source of background noise emanating from the silver-coated surface is a bright, but short-lived luminescent blinking that is produced by the silver nanoparticles, an observation which we designate "silver storms." These silver storms have been previously observed for both gold and silver nanoparticles, and remain an interesting phenomenon [21, 22, 41, 57]. Peyser et al. have indicated that the silver storms strongly occur at wavelengths <520 nm. However, we have observed these storms using evanescent excitation via a total internal reflection (TIR) microscope with near-IR excitation at 680 nm, one of the excitation wavelengths currently used in our Odyssey imagers [57]. To view a movie of these silver storms, see http://www.licor.com/silverstorm. Because the Odyssey scans large areas over long time periods, it is not possible to observe silver storms in movie format. However, we believe storms likely occur and contribute to background noise in Odyssey images, particularly since excitation power is greater in the Odyssey than in our microscopic observations (1,000 W/cm^2 vs. 10 W/cm^2). To further investigate silver storms, we have made observations using two-photon excitation. This setup allowed the emission spectrum to be obtained at visible wavelengths without interference from the near-IR excitation light. It also allowed emission lifetimes to be measured, in order to distinguish between prompt scatter and delayed emissions. The two-photon excitation work was performed at the Nebraska Center for Cell Biology at Creighton University, Omaha, NE.

7.2 Two-Photon Microscopy Imaging of Silver Nanoparticles

Silver nanoparticles were deposited by reduction of silver ion with DMF [56] on ITO-coated coverglass (ZC&R, 140 Ω/sq). Silver storms were observed under two-photon excitation as shown in Fig. 9.

Silver nanoparticles were imaged using intense near-IR illumination at 740 and 950 nm by two-photon laser scanning microscopy. Femtosecond pulses of near-IR illumination from a tunable Chameleon XR laser (Coherent Inc., Santa Clara, CA) were scanned across the sample by an LSM510 META NLO laser scanning microscope with a 63× Plan Apochromat 1.4 NA oil immersion objective

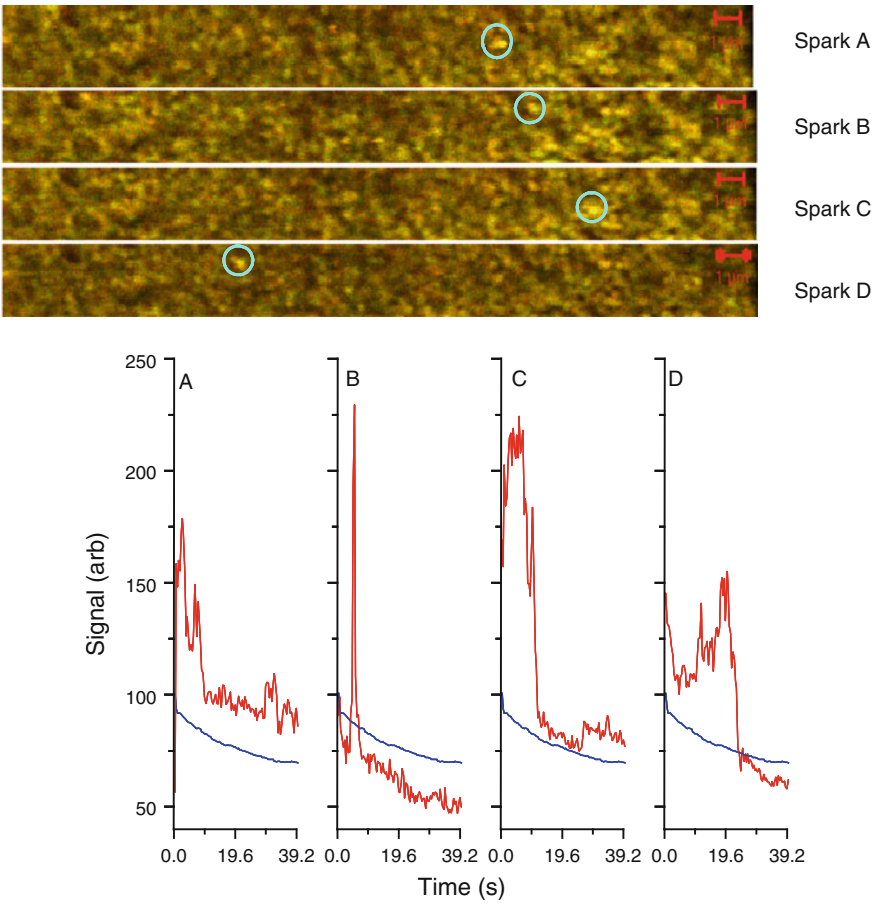

Fig. 9 Silver nanoparticles "sparking" on ITO-coated glass coverslips. A 2.9 × 29 μm region was imaged at a frame rate of 2.55 Hz. The *blue line* indicates the average pixel intensity for the entire image, while the *red lines* show the average pixel intensity in the sparking regions circled in the frames shown above. Scale bar is 1 μm

(Carl Zeiss Inc., Thornwood, NY). The repetition rate of the pulse train was 90 MHz. We estimate the spatial resolution to be approximately 0.3 μm radially (in the image plane) by 0.75 μm axially (depth of the imaging plane). An average laser power of approximately 0.4 mW was directed to the sample for most of the measurements. The light emitted from the sample was initially separated into two detection channels using a 500-nm long pass dichroic (500 DCXR, Chroma Technology, Brattleboro, VT) and detected by photomultiplier tubes without descanning. Blue emission was isolated using a custom-made bandpass filter (HQ460/80, Chroma Technology, Brattleboro, VT) and green emission was isolated using an HQ540/60 bandpass filter (Chroma Technology, Brattleboro, VT).

7.3 Silver Storm Emission Spectra

To obtain emission spectra from individual pixels, the emission was diverted to a diffraction grating and detected in 24 wavelength bands centered from 404 to 650 nm using the META detector of the LSM510 microscope. The spectral resolution was approximately 10.8 nm. No attempt was made to measure or correct for any nonuniform spectral response of the META detector. The emission results from the silver nanoparticles for both 740 and 950 nm two-photon excitation show that there is a broad emission spectra from the silver nanoparticles, throughout the 400–650 nm range (Figs. 10 and 11). The emission spectra may well continue into the near-IR with the instrumentation having a detector limit of 650 nm. These results are consistent with other reported data showing a broad emission spectra from silver nanoparticle excitation [22, 57].

7.4 Silver Storm Lifetime Measurements

To perform lifetime imaging, the blue emission was diverted and detected by a H7422-40 GaAs photomultiplier detector (Hamamatsu Corp., Bridgewater, NJ) and the emission lifetime was measured by Time Correlated Single Photon Counting using a Becker and Hickl SPC 830 card (Becker and Hickl GmbH, Berlin, Germany), synchronized to the laser pulses and the LSM510 scan signals. The field was scanned approximately three times and photons accumulated for 90 s. To avoid double pulse counting artifacts, the laser power was reduced so that much less

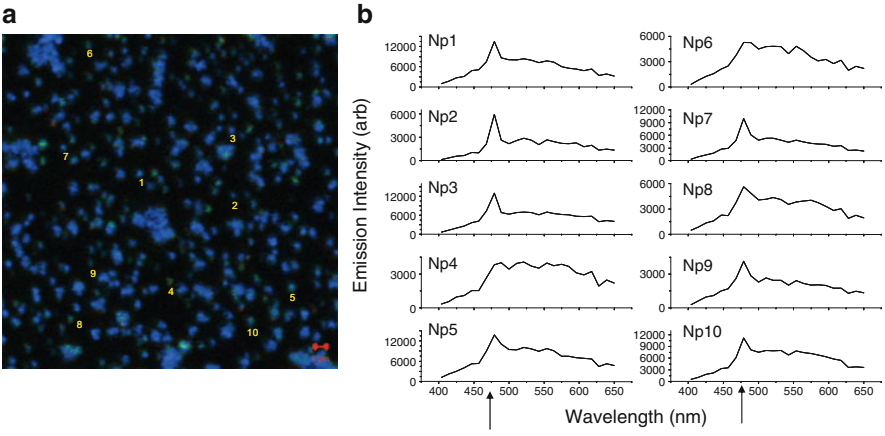

Fig. 10 (**a**) Spectral image showing blue emission from silver nanoparticles using 950 nm two-photon excitation. Scale bar is 1 μm. Spectra from individual nanoparticles are shown in (**b**). SHG and Hyper-Raleigh scattering expected at 475 nm (*arrow*). The continuous spectrum is probably silver-ion luminescence. All spectra are background subtracted

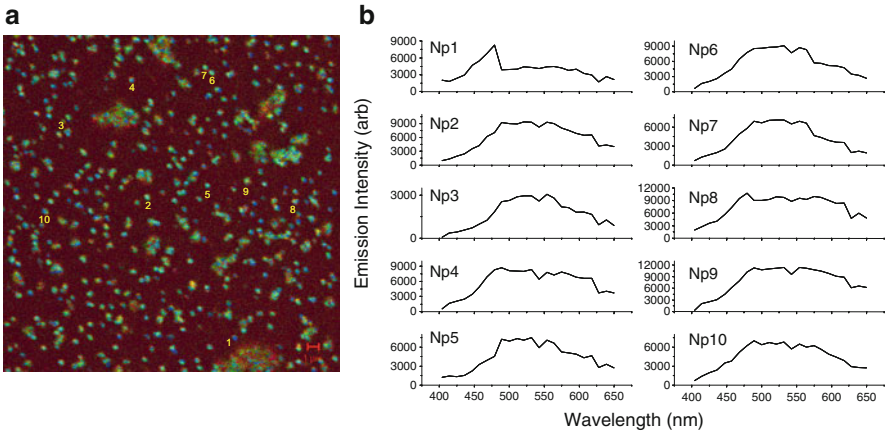

Fig. 11 (**a**) Spectral image showing emission from silver nanoparticles using 740 nm two-photon excitation. Scale bar is 1 μm. Spectra from individual nanoparticles are shown in (**b**). SHG and Hyper-Raleigh scattering expected at 370 nm, and not detectable in the spectra. The continuous spectrum is probably silver-ion luminescence. All spectra are background subtracted

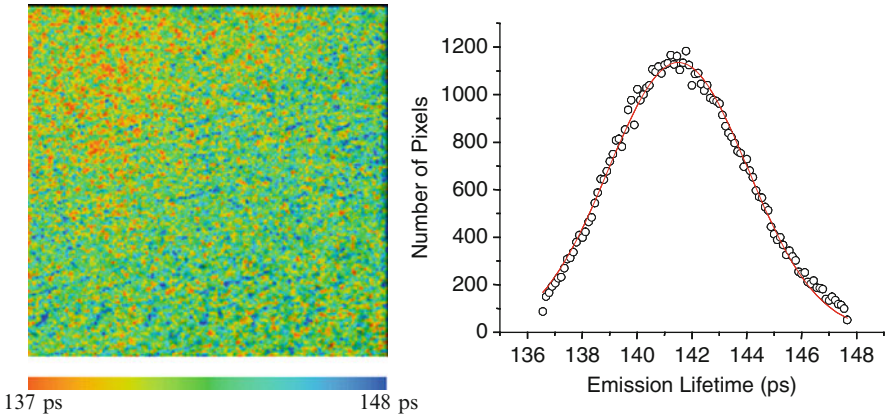

Fig. 12 Lifetime measurements for silver nanoparticle emissions using two-photon excitation. A single Gaussian fit to lifetime histogram gives an average emission lifetime of 141 ± 5 ps

than one photon was detected per pulse. Photon count rates did not exceed 1 MHz. The analysis of the lifetime measurements was performed using the Becker and Hickl SPC Image Software. The lifetime measurement fit is a convolution of the instrument response function (assumed Gaussian) and a single exponential decay. FWHM of the IRF is estimated to be 196 ps from the same fit. The results from the lifetime measurements show that the silver nanoparticles display a very short (140 ps) lifetime (Fig. 12). We believe that this may be the first reporting of the emission lifetimes for these silver storms.